Indian Journal of Chemistry
Vol. 57A, July 2018, pp. 896-904

Prussian blue/ superactivated carbon composite-modified electrode for detection of *p*-phenylenediamine

Lin Hu*, Jin qing Li*, Xiao qin Zhou, Tong tong Bai, Qu jin Cui, Juan Tang & Wen yuan Xu

School of Materials Science and Engineering, East China Jiao Tong University, Nanchang, Jiangxi, 330013, PR China

Email: 1604815540@qq.com/ hulin21@hotmail.com (LH)

Received 19 March 2018; revised and accepted 18 June 2018

A novel approach for the selective determination of *p*-phenylenediamine in aqueous solution using Prussian blue (PB)/ superactivated carbon (SAC) composite-modified glassy carbon electrodes is reported. The chemical constitution and microstructure of PB/SAC composites are studied by SEM, BET and IR data. Due to its unique structure and properties originating from Prussian blue in the superactivated carbon frame, PB/SAC composites show high electrocatalytic activity towards the oxidation of *p*-phenylenediamine. A special chemical reaction and electron transfer process on the surface of PB/SAC composite-modified GC electrode is proposed and evaluated by cyclic voltammetry and AC impedance in the presence of *p*-phenylenediamine. The current value of differential pulse voltammetry increases linearly with the *p*-phenylenediamine concentration in the range 2×10^{-7}–1×10^{-3} M with a detection limit of 6.47×10^{-8} M (S/N = 3). The relative standard deviation of the waste water samples is < 6% and the recovery rate is 97−104%. These results suggest that the modified electrode has high selection for *p*-phenylenediamine, good repeatability, and operational stability. The modified electrode has been successfully used to analyze the amount of *p*-phenylenediamine in water samples.

Keywords: Electroanalytical chemistry, Electrodes, Modified electrodes, Glassy carbon electrodes, Superactivated carbon, Cyclic voltammetry, *p*-Phenylenediamine, Prussian blue

The aromatic amine, *p*-phenylenediamine (PPD) is widely used as a component in polymers, pigments, hair dyes and textile products. It is toxic, and if its content in clothing or water is greater than the national standard (0.5–2.0%)[1], it causes damage to the human body[2]. It is estimated that 0.06%–0.2% *p*-phenylenediamine in cosmetic and non-food products will irritate and stimulate the skin. Keratin in the hair has a strong affinity to *p*-phenylenediamine, and when *p*-phenylenediamine has long-term contact with the skin, it can cause skin cancer. It can also cause irritation when it comes in contact with eyes[3,4]. Furthermore, residual *p*-phenylenediamine in industrial waste water is highly poisonous to aquatic organisms, resulting in long-term adverse effects in the environment. Government regulations have called for the levels of *p*-phenylenediamine in waste water to be below a certain low ppm level to ensure that the local aquatic species are not endangered[5]. Some conventional analytical techniques have been used in the detection of PPD, including high-performance liquid chromatography (HPLC)[6,7], gas chromatography (GC)[8], and gas chromatography–mass spectrometry (GC-MS)[9,10]. However, these methods have some limitations, such as restriction in the GC determination of highly polar and low-volatility substances, and the mobile phase of HPLC requiring the use of 1,8-diaminooctane or triethylamine as an amine modifier and sodium heptane sulfonate as a counter ion to solve asymmetric and tailing peaks[11,12]. Therefore, development of an accurate and inexpensive method for the detection of *p*-phenylenediamine is urgently needed.

In recent times, different modified electrodes have been used to detect PPD or other analogues. Sasikumar *et al.*[13] developed a highly sensitive *o*-phenylenediamine (OPD) sensor based on Fe_3O_4-doped functional multiwalled carbon nanotubes (Fe_3O_4@f-MWCNT) composite fabricated on a glassy carbon electrode, their results showed a wide linear range of removal at OPD concentrations of 0.6–80 mM. Guo[14] simultaneously determined hydroquinone and catechol using a pyridinic nitrogen-doped graphene (pyridine-NG) modified electrode, the detection limit is as low as 0.38 μM for hydroquinone and 1 μM for catechol (S/N = 3). A modified graphene paste electrode with a ferrocene-derivative has been constructed[15], and the results showed that the square wave voltammetric peak current of hydroxylamine

increased linearly with the hydroxylamine concentration in the range of 2.0×10^{-7} to 2.5×10^{-4} M. These studies showed that the modified electrode has wide applications. These methods showed good detection results, however, they also have some inherent limitations. The layered structure of graphene or graphene oxide contributes to excellent electrochemical performance of the modified electrode, but it is expensive and hard to obtain[15,16]. The modification of electrodes with multiwalled carbon nanotubes can greatly improve the electron transfer reaction, but the reproducibility is not good, and the cost is high[17-19]. Therefore, it is important to find a substitute material that has the advantages of a modified electrode while avoiding its drawbacks.

Superactivated carbon (SAC) is a rich and inexpensive source of raw materials. It has extraordinary electrical conductivity, high chemical stability, excellent mechanical strength and a high surface-to-volume ratio, which endows it with wide adaptability in the field of electrochemistry[20,21]. As a porous carbon material, superactivated carbon has a developed pore structure and large surface area, which provides it a high adsorption capacity. Thus, it can effectively adsorb and disperse Prussian blue, ($Fe_4[Fe(CN)_6]_3$), and other auxiliary substances. Prussian blue (PB) has the advantages of electrochemical reversibility, high stability, and low price, and has been generally used as an 'artificial peroxidase' in electrochemical sensors[22,23]. Herein, we report the fabrication of a Prussian blue/ superactivated carbon composite-modified glass carbon electrode and then detection of trace amounts of *p*-phenylenediamine, using the modified glassy carbon electrode (PB/SAC@GCE).

To the best of our knowledge, no study has reported the detection of *p*-phenylenediamine by using superactivated carbon-modified glassy carbon electrodes.

Materials and Methods

Superactivated carbon was prepared in our lab as per the procedure described *vide infra*, *p*-phenylenediamine, Al_2O_3 powder, polyvinylidene fluoride (PVDF) and graphite powder were purchased from Aladdin Company (Shanghai, China). Nafion solution (15%) was obtained from Sigma (St. Louis, MO, USA), and was directly used. $Na_2HPO_4\cdot12H_2O$ (AR) and NaH_2PO_4 (AR) were obtained from Xi Long Chemical industry (Guangdong, China). All chemicals were of analytical grade and solutions were prepared with doubly distilled water.

All electrochemical measurements were performed on a CHI630D electrochemical workstation with the software package provided with it (Shanghai, China). A three-electrode system including a bare glassy carbon electrode (GCE, 3 mm in dia., model MF-2012, BAS) or modified GCE as the working electrode, a saturated calomel electrode as the reference electrode, and a platinum wire as the auxiliary electrode were used in this setup. The FTIR spectra were recorded on an IRAffinity-1 Fourier transform infrared spectrophotometer (Thermo Fisher/ Finnigan-Cahn-Nicolet, USA). The various solutions were prepared with a PHS225 pH meter (Shanghai, China). A temperature magnetic stirrer (Jintan, China) was used to disperse the raw materials and promote the formation of the composites. The ultrasonic process was carried out by a KQ-500 Bonifier (Kunshan, China).

Preparation of superactivated carbon

The raw material of superactivated carbon, i.e., coconut shell, was collected from a supermarket, crushed, washed with doubly distilled water, and dried. To remove the non-carbon elements and volatile substances, the dried material was carbonized in a box-type atmosphere furnace. After cooling to room temperature, the activated carbon raw material was mixed with solid KOH in 1:5 mass ratio, ground into a powder and activated at 1128 K for 70 minutes in a box-type atmosphere furnace. The resulting material was soaked in dil. hydrochloric acid and then washed repeatedly with doubly distilled water until the pH of the superactivated carbon reached 6. Next, it was dried in an oven at 393 K for 12 h and finally stored in bottles.

Preparation of PB/SAC composite material

Accurately weighed Prussian blue was added into a beaker containing alcohol with stirring. When PB was completely dissolved, dried superactivated carbon was added and ultrasonically dispersed for 10 minutes, before being continually stirred for half an hour. Expanded graphite powder was added and stirred for another hour. The ratio of PB:SAC expanded : graphite was kept as 1:2:7. Lastly, 15% polyvinylidene fluoride (PVDF) was added, and the mixture was sonicated for 1 h for even distribution in the composite material and further stirred for 5 h at room temperature (the mixture was kept away from light).

Preparation of PB/SAC-modified glass carbon electrode (PB/SAC@GCE)

A bare glassy carbon electrode was polished with 1, 0.3, and 0.05 μm aluminium oxide powder in the same direction on wet suede. Ultrasonic cleaning was performed for 10 minutes with ethanol and distilled water, and then, the electrode was dried naturally. Then 10 μL of prepared PB/SAC composite was pipetted on the polished bare glassy carbon electrode, spread evenly and dried under natural conditions. Further 5 μL of a 15% Nafion solution was pipetted using a micro-injector, dispersed onto the surface of the PB/SAC composites at room temperature and dried naturally. The PB/SAC-modified electrode was placed in a buffer solution (pH 7.0) until the composite formed a layer of polymer film. Then, the potential was reduced for one minute, and the PB/SAC@GCE was obtained.

Results and Discussion

Characterization of superactivated carbon and PB/SAC composite

The typical morphology of superactivated carbon was characterized by scanning electron microscopy (Fig. 1a&b). The SEM image shows its coarse and porous structure. It can be seen that the external surface of the superactivated carbon has cracks and crevices, and some grains in various sizes in large holes, which demonstrates that a porous structure was formed during carbonization and activation, as most of the organic volatiles had evaporated, leaving behind a ruptured surface of the activated carbon with numerous pores. Spherical particles of PB can be clearly observed on the surfaces and pores of superactivated carbon (Fig. 1c&d). The spherical particles may be Prussian blue with special cubic structure coated with graphite powder. These spherical particles are equipped with the ability to transfer electrons since the iron element of Prussian blue has variable valence.

The nitrogen adsorption/desorption isotherms of the superactivated carbon and PB/SAC composition at 77 K and the corresponding pore size distribution are shown in Fig. 2. According to the IUPAC classification, the isotherms of superactivated carbon can be identified as type I, confirming the microporous character. SAC exhibits a BET surface area of 2760.4 m^2/g, which is far more than that of the active carbon commonly available in the market and is also slightly better than the theoretical value for graphene[24]. It has a mean pore size of 1.968 nm, which is much smaller than the pore size of activated carbon reported in literature[25,26], and is more favourable for dispersion of Prussian blue and expanded graphite powder. The BET surface area of PB/SAC composite is 2746.5 m^2/g, and is not much different in comparison with that of SAC.

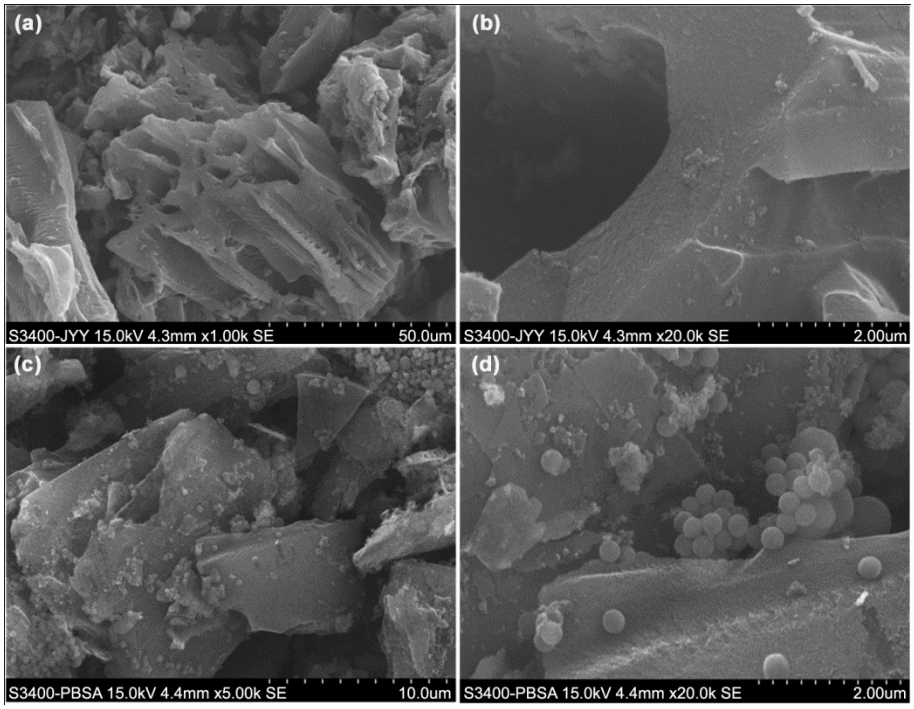

Fig. 1 — (a, b) SEM images of superactivated carbon, and, (c, d) SEM images of PB/SAC composite.

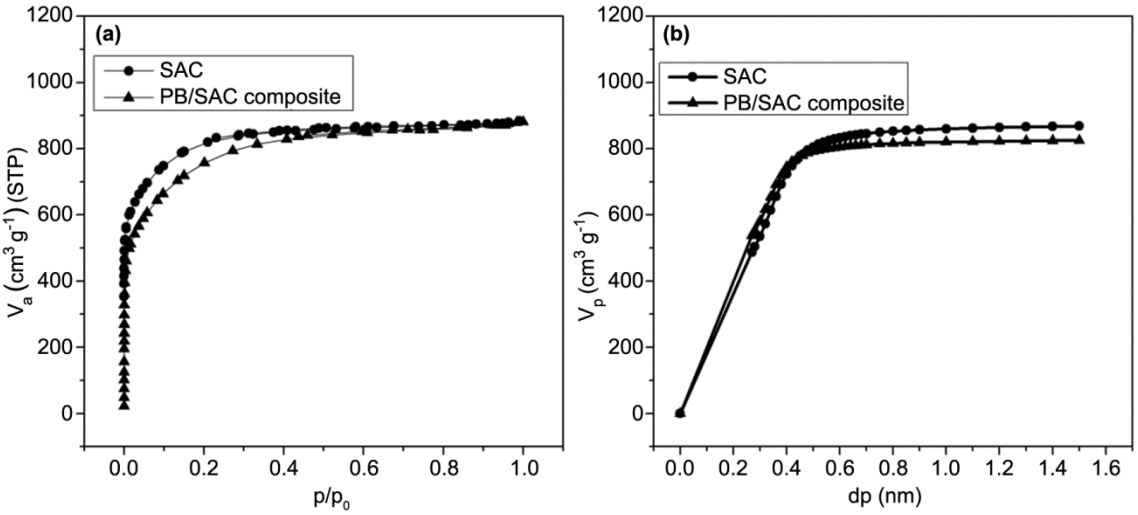

Fig. 2 — (a) Nitrogen adsorption/desorption isotherms, and, (b) pore size distribution curves of SAC and PB/SAC composite.

SAC disperses the Prussian blue as well as increases the contact area of the reaction, thereby reducing the impedance of the modified electrode.

Optimization of the best proportion of PB/SAC composites

The electrochemical properties and resistance of the modified electrode vary with the composition of the PB/SAC composites. To select the modified electrode with the best electrochemical performance and least resistance, the proportion of PB/SAC composites was optimized. The composites were prepared according to the method described above, and the glassy carbon electrode was modified in the same manner. Cyclic voltammetry (CV) was measured at the surface of a modified electrode in a 1×10^{-5} M *p*-phenylenediamine solution (*p*H = 7.0) at a scan rate of 0.05 V/s (Fig. 3).The different composites are shown in Table 1.

The electrode, T_0, has only an anodic current peak, indicating that it is an irreversible electrode, while the electrode T, exhibited had more significant redox peaks compared to the T_0 electrode (Fig. 3(a), curve 1), indicating that the superactivated carbon plays a very important role in improving the electrochemical properties of the electrodes. This is because activated carbon has a very large specific surface area and developed pore structure that adsorbed PB in large quantities, resulting in better transmission of the electrons. The cyclic voltammetric current of a bare GCE was extremely small and there were no redox peaks (Fig. 3(b), curve 4). There is no obvious redox peak in the CV diagram when there is no PPD in the solution (Fig. 3(a), curve 3), which shows that it is easy

Table 1 — Composition of the composites

Electrode	Prussian blue (g)	Superactivated carbon (g)	Expanded graphite powder (g)	PVDF (%)
T	0.01	0.02	0.07	15
T_0	0.01	0.00	0.07	15
T_1	0.01	0.02	0.07	5
T_2	0.01	0.02	0.07	10
T_2	0.01	0.02	0.07	15
T_3	0.01	0.02	0.07	20
T_4	0.02	0.02	0.07	15

to lose PPD or obtain electrons on the surface of the electrode and trigger oxidation-reduction reaction. It has been shown that the $\triangle E_p$ ($\Delta E_p = E_{pa}–E_{pc}$) is inversely proportional to the electron transfer rate, and smaller the ΔE_p (0.314 V), the better is the reversibility of the electrode T[27]. It can be observed from Fig. 3(c) and 3(d) that the separation peak (ΔE_p) of curve 1 is the smallest and has obvious redox peaks. Thus, the optimum composition of Prussian blue, superactivated carbon and expanded activated carbon is 0.01:0.02:0.07.

AC impedance (EIS) is an accurate tool used to analyse the electrical properties of an electrode/electrolyte interface. The EIS data was recorded in a 1×10^{-5} M PPD solution (Fig. 4), with the following parameters: initial potential, 0 V; maximum frequency, 1.5×10^6 Hz; minimum frequency, 0.05 Hz; and amplitude, 0.005 V.

The inset of Fig. 4 shows the equivalent circuit diagram for this system, where R_Ω represents ohmic resistance presented by the bulk solution, Z_f is Faradaic impedance, which can be divided into electron transfer resistance R_{ct} (high frequency) or diffusion resistance

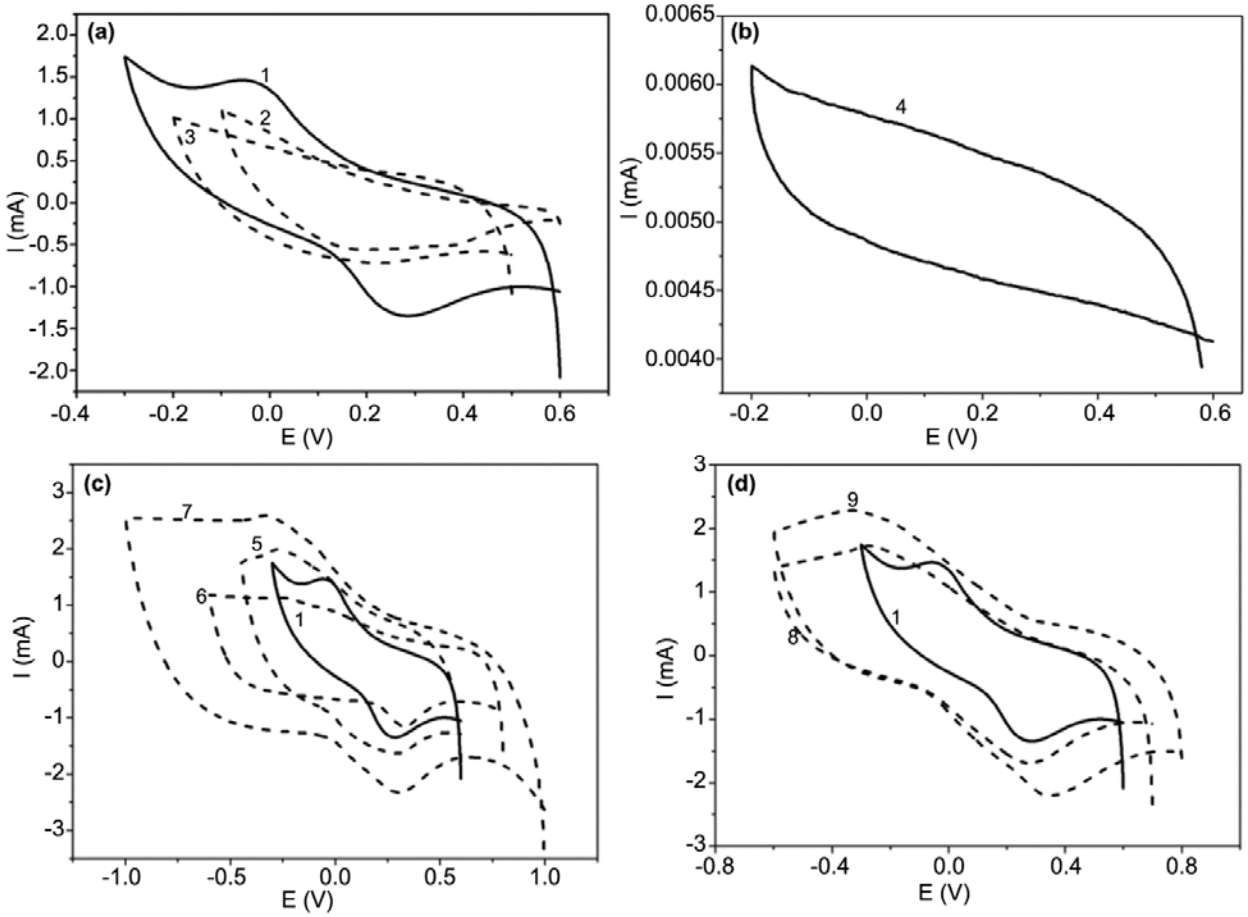

Fig. 3 — Cyclic voltammograms of the modified electrodes. [(a) T and T_0 electrodes with 1×10^{-5} M PPD (curves 1, 2), T electrode with 0.0M PPD (curve 3); (b) bare electrode with 1×10^{-5} M PPD (curve 4); (c) T, T_1,T_2 and T_3 electrodes (curves 1, 5, 6, 7) with 1×10^{-5} M PPD; (d) T, T_4, T_5 electrodes (curves 1, 8, 9) with 1×10^{-5} M PPD in phosphate buffer (pH 7.0, 0.1 M). Scan rate, 50 mV/s. Since the redox peak values of different composites are different, the optimal coordinate range is shown to make the graph clearly visible].

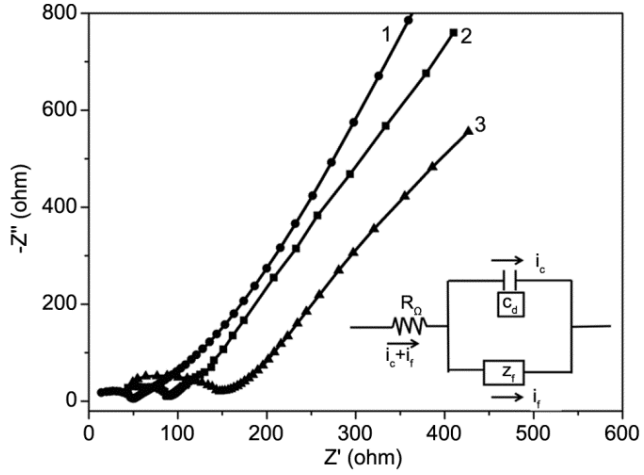

Fig. 4 — AC impedance spectra of the (1) PB/SAC-modified electrode, (2) PB/graphite-modified electrode, and (3) graphite-modified electrode in 0.1 mol/L PBS buffer solution (pH 7.0) containing 1×10^{-5} mol/L PPD. [Inset: Equivalent electrical circuit of a three-electrode cell].

Z_w (low frequency). The impedance spectrum consists of a semicircle in the high frequency region and a straight line in the low frequency region. The semicircle in the high frequency region reflects the charge transfer resistance (R_{ct}), and the straight line in the low frequency region reflects the Warburg impedance (Z_w)[32].

In the high frequency region, the resistance of graphite-modified electrode, PB/graphite-modified electrode and PB/SAC modified electrode was 150 Ω, 100 Ω and 50 Ω, respectively (Fig. 4), which shows that the electron transfer rate of the PB/SAC composites modified electrode is greatly reduced due to the porous structure and large surface area of the SAC, which has fully dispersed the Prussian blue, a favourable electron conductivity agent. This shows that the transfer ability of electron in the PB/SAC modified electrode has been significantly improved.

Infrared analysis of PB/SAC composites

As shown in Fig. 5, the FTIR spectra display several absorption peaks; the bands at 1575 cm^{-1} and 1650 cm^{-1} represent the bonded C=C group of alkene (Fig. 5 (curves 2&3)). The sharp band at 2050 cm^{-1} assigned to the C≡N stretching vibration remains unchanged, showing that the C≡N bond in Prussian blue is unchanged during the preparation of the composite[27]. The bands 1500 and 1400 cm^{-1} are assigned to the C-C stretching, and the broad band at approximately 3425 cm^{-1} is ascribed to the N-H stretching vibration, from SAC[29, 30]. The infrared spectra of the PB/SAC composites showed that some of the raw material still existed as the individual components. The combination of the intrinsic properties of the components results in the improved performance of the modified electrode.

Influence of pH

The electrochemical behaviour of PPD is dependent on the pH value of the aqueous solution, whereas the electrochemical properties of PB/SAC@GCE are independent of pH. Therefore, optimization of pH seems to be necessary in order to obtain the optimum electrocatalytic oxidation of *p*-phenylenediamine. Thus, the electrochemical behaviour of *p*-phenylenediamine was studied in different pH values (5.5<pH<8.0) at the surface of PB/SAC@GCE by the DPVs.

With the increase in pH, the cathodic peak current of *p*-phenylenediamine increased initialy and then decreased; the cathodic peak was the largest when the pH value was 7.0 (Fig. 6). PPD gains and loses electrons on the surface of the electrode, and the neutral condition facilitates this process because of absence of interference by H^+ or OH^-. The electrocatalytic oxidation of PPD at the surface of PB/SAC@GCE was more favored under neutral conditions than in acidic or basic medium[31]. Thus, a pH of 7.0 was chosen as the optimum pH for the electrocatalysis of *p*-phenylenediamine oxidation at the surface of PB/SAC@GCE.

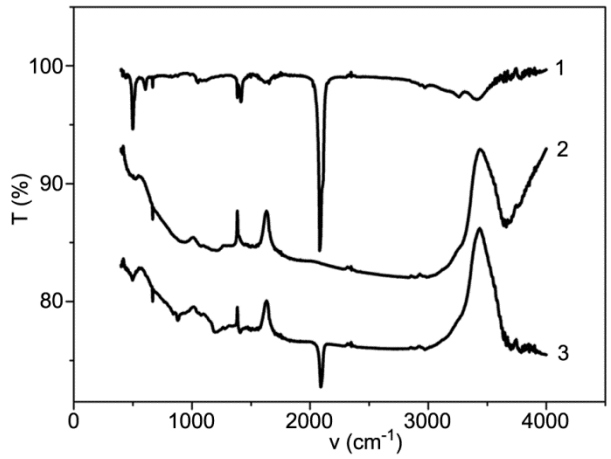

Fig. 5 — The infrared spectra of PB (curve 1), SAC (curve 2), and PB/SAC composite (curve 3).

Electrocatalytic oxidation of PPD at PB/SAC@GCE

The effect of scan rate on the electrocatalytic oxidation of PPD at the PB/SAC@GCE was investigated by CV (Fig. 7). The parameters of cyclic voltammetry are as follows: the initial potential, 0.6 V; maximum potential, 0.6 V; minimum potential, –0.2 V; number of scans, 2; sampling interval, 0.001 s; and sensitivity, 0.001.

As observed from Fig. 7, the anodic peak potential shifts to more positive values with an increase in the scan rate from 0.1 to 10 mV/s, while the cathodic peak shifts more negatively. This confirms the kinetic limitation in the electrochemical reaction. A good linear correlation (R^2 = 0.998) was acquired between the peak currents (I_p) and square root of the scan rate ($v^{1/2}$), indicating that the process is diffusion controlled rather than surface controlled at a sufficient overpotential.

Differential pulse voltammetry (DPV) is a more sensitive technique for the detection of the electrochemical oxidation of PPD than CV. The DPV response of PB/SAC@GCE was determined with the addition of PBS (pH = 7.0) containing varying concentrations of PPD. The parameters of DPV were as follows: initial *E* (V) = –0.6; final *E* (V) = +0.6; increment *E* (V) = 0.005; amplitude (V) = 0.05; pulse

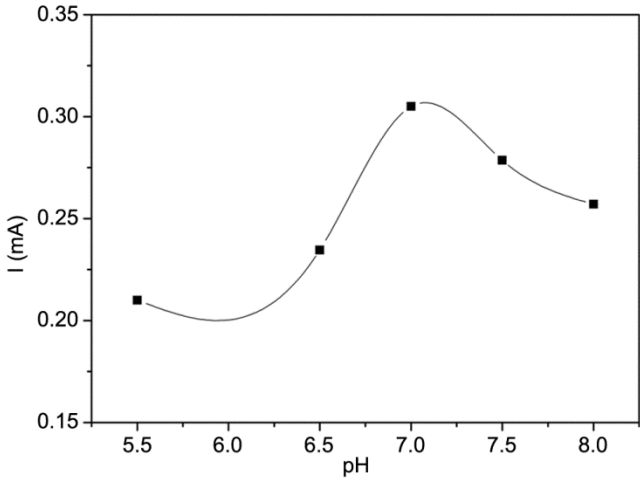

Fig. 6 — Electrocatalytic peak current obtained from DPVs at varying pH (5.5–8.0) containing *p*-phenylenediamine (1×10^{-5} mol/L).

width (s) = 0.05; sampling width = 0.04; pulse period (s) = 0.1; quiet time (s) = 30; and sensitivity (A/V) = 1×10^{-4}.

Figure 8(a) shows that the cathodic peak values gradually increase with the increase in the PPD concentration. The PPD concentration increases in a certain range, its diffusion rate in the test solution and adsorption rate on the PB/SAC@GCE electrode increase; thus, the peak current value increases. When the PPD concentration is notably small (2×10^{-7} mol/L), the cathodic peak current value remains at –0.8520 mA, which indicates that the PB/SAC@GCE electrode has high sensitivity in PPD detection.

As shown in Figure 8(b), in the range of 2×10^{-7} to 1×10^{-3} M, there is a good linear relationship between the cathodic peak and the logarithm of the PPD concentration [I_{pa} (mA) = $(-1.489\times10^{-3})\times\ln c - 0.5319$; R^2 = 0.961]. The detection limit being three times the standard deviation, the limit of detection of the PB/SAC@GCE electrode is 6.47×10^{-8} mol/L.

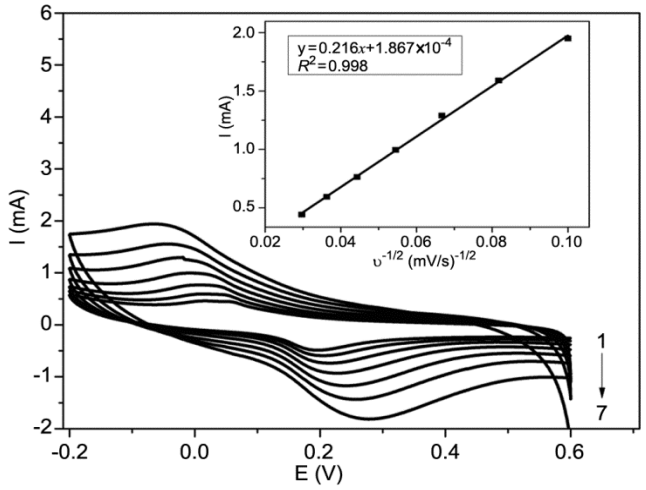

Fig. 7 — Cyclic voltammograms of the PB/SAC-modified electrode in a 0.1 mol/L PBS buffer solution (pH = 7.0) containing 1×10^{-5} mol/L PPD at a scan rate of 0.1–10 mV/s. [The inset is a plot of redox peak current versus square root of scan rate].

Being electroactive, *p*-phenylenediamine (PPD) can be electrooxidized and/or electroreduced at modified or glassy carbon electrodes. Superactive carbon with a rich pore structure will disperse Prussian blue, which is a good electronic conductor, thus, PB/SAC composites can greatly improve the sensitivity of the electrode. Therefore, PPD can be detected more effectively.

Interference study

The interference of various ions was verified under optimal conditions with 1×10^{-5} M *p*-phenylenediamine (pH 7.0). These are commonly found in aqueous solutions or waste water samples. To verify the interference in the detection of *p*-phenylenediamine, K^+, Cl^-, Na^+, NO_3^-, glucose, ascorbic acid, or ethanol (100-fold excess each) or Ag^+, Zn^{2+}, Pb^{2+}, Mg^{2+}, Mn^{2+}, Co^{3+}, Cr^{2+}, and SCN^- (200-fold excess each) were added to the phenylenediamine solution. Approximately ±4% relative error in the cathodic peaks of DPV was observed, which indicates that these interfering ions have no effect on the determination of *p*-phenylenediamine on PB/SAC@GCE. Therefore, we can conclude that the interference of most of these ions on the detection of *p*-phenylenediamine is negligible, and thus, we can detect *p*-phenylenediamine by PB/SAC@GCE.

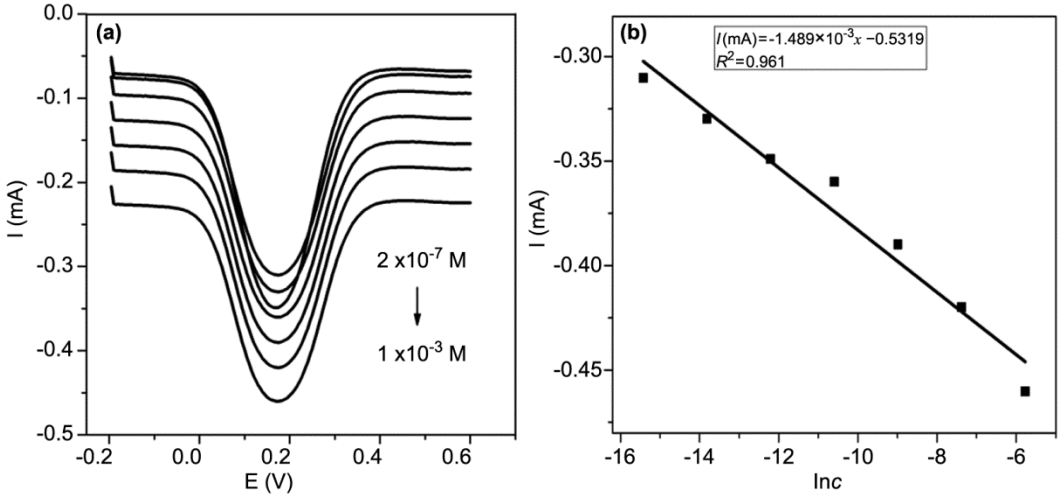

Fig. 8 — (a) Differential pulse voltammograms of PPD at different concentrations (1–7 = 1×10^{-3} to 2×10^{-7} M); (b) Linear relationship between the oxidation peak current and the logarithm of the PPD concentration.

Recovery rate of *p*-phenylenediamine

To assess the accuracy of the present electrochemical analytical method, the method was applied for the determination of *p*-phenylenediamine in water samples. First, 10 mL of the water sample was diluted to 50 mL with a 0.1 M PBS solution (pH = 7.0), and a series of 50 mL water samples was prepared. Varying amounts of *p*-phenylenediamine was added to the water samples, and the DPV was recorded for the solutions. Five parallel experiments were carried out simultaneously. The results for determination of the *p*-phenylenediamine in the real samples are given in Table 2. The recovery rate of the method is 98–102%, which indicates the reliability of the proposed method.

Application

To test the applicability of the method, waste water samples from textile mills were stored in a brown glass bottle, and tested within 24 h. Initially, the waste water sample was filtered to remove suspended impurities, and diluted by a stepwise solution method to obtain varying concentrations of *p*-phenylenediamine in the water samples. The results are show in Table 3. Five parallel experiments were carried out simultaneously. The relative standard deviation of the five groups of samples did not exceed 6%; the recovery rate was 97–104%, which indicates that this test method has good stability and repeatability. It has a certain operability and can be applied to the actual *p*-phenylenediamine detection.

Comparison with other methods

Electrochemical techniques are suitable for miniaturization, have better sensitivity compared to optical detection techniques, and their components can be reliably microfabricated, and are therefore, widely used[33]. Bai[34] *et al.* determined *p*-phenylenediamine in hair dye using β-MnO_2 nanowires modified glassy carbon (GC) electrodes. Hudari[17] *et al.* simultaneously detected *p*-phenylenediamine (PPD) and resorcinol (RSN) with composites of multiwalled carbon nanotube, wherein oxidation was carried out at +0.17 and +0.61 V, respectively. Dai[35] *et al.* successfully synthesized nitrogen doped graphene (NG) modified GCE, which showed electrocatalytic activity towards the oxidation of PPD. Zhu *et al.*[36] prepared a photoelectroactive film that can detect PPD under visible light.

Table 4 summarizes comparision of the present electroanalytical determination of PPD with other

Table 2 — Determination of *p*-phenylenediamine in the water samples

Sample	PPD (mol/L) Added	Found	Recovery (%)	RSD (%)
Distilled water	0	0	-	-
	5×10^{-6}	4.9×10^{-6}	98	3.2
	1×10^{-5}	1.03×10^{-5}	103	1.9
	1.5×10^{-5}	1.52×10^{-5}	101.3	2.4
Tap water	0	0	-	-
	7.5×10^{-6}	7.6×10^{-6}	101.3	2.2
	1.25×10^{-5}	1.23×10^{-5}	98.4	3.5
	1.75×10^{-5}	1.81×10^{-5}	103.4	1.8

Table 3 — Determination of PPD in waste water samples[a]

Sample	PPD (mol/L) Present[b]	Found	RSD (%)	Recovery (%)
1	2.5×10^{-5}	2.47×10^{-5}	4.3	98.8
2	5×10^{-5}	4.86×10^{-5}	5.1	97.2
3	1×10^{-5}	1.04×10^{-5}	3.8	104.0
4	2×10^{-4}	2.07×10^{-4}	2.4	103.5
5	4×10^{-4}	3.88×10^{-4}	4.6	97.0

[a]Waste water samples were provided by the textile mills.
[b]Intial conc.: 0.25 mg/L as shown by HPLC analysis (according to GB/T24800.12-2009).

Table 4 — Comparison of various methods for determination of PPD

Sensor	Linear range (M)	Detection limit (M)	RSD (%)	Method[Ref.]
PB/SAC composites modified	2×10^{-7} to 1×10^{-3}	6.47×10^{-8}	3.5	This work
β-MnO_2 nanowires modified GCE	2×10^{-7} to 1.5×10^{-4}	5×10^{-8}	3.9	Amperometric[34]
Mutiwalled carbon nanotubes with chitosan composites /GCE	5.08×10^{-6} to 1.96×10^{-4}	5×10^{-8}	2.4	Linear sweep voltammetry[17]
Nitrogen doped graphene modified GCE	2×10^{-6} to 5×10^{-4}	6.7×10^{-7}	-	Linear sweep voltammetry[35]
CdS and graphene sheets coated on F-doped SnO_2 modified GCE	1.0×10^{-7} to 3.0×10^{-6}	4.3×10^{-8}	2.0	Photoirradiation-cyclic voltammogram[36]
Fe_3O_4 doped with functionalized multiwalled carbon nanotubes composite fabricated GCE[13] for detection of *o*-phenylene diamine	6×10^{-7} to 8×10^{-5}	5×10^{-5}	-	Differential pulse voltammetry

reported methods. The assembled PB/SAC electrode in the present study has a simple structure, is easy to manufacture at a low cost, and can provide a wide linear range and a low detection limit.

Conclusions

In this work, superactivated carbon was first used to modify electrodes. Superactivated carbon has a well-developed porous structure and an ultra-high specific surface, and can effectively adsorb and disperse PB. The, PB/SAC composites exhibited electrocatalytic properties, good sensitivity and selectivity, and an enrichment ability, which significantly catalyses the redox reaction of PPD. The electrochemical behaviour of *p*-phenylenediamine on the PB/SAC@GCE is described in detail. The cathodic peaks (I_{pa}) at the potential around –0.10 V of DPV had a linear relationship with the logarithm of the concentration (lnc) of PPD within the range 2×10^{-7} to 1×10^{-3} M with a detection limit (3σ) of 6.47×10^{-8} M. Finally, this method has good repeatability for the determination of PPD in water samples, and a certain operability and can thus be applied for detection of *p*-phenylenediamine in practical situations. The present work demonstrates that superactivated carbon is a promising electrode material for the electrochemical determination of PPD and other similar aromatic amines in environmental analysis.

Acknowledgement

This work was supported by the National Natural Science Foundation of China (Nos. 21563011).

References

1 Pot M, Coenraads J, Blömeke B, Puppels J & Caspers J, *Contact Dermatitis*, 74 (2016) 152.
2 De Boeck M, van der Leede B-J, De Vlieger K, Geys H, Vynckier A, Van Gompel J, *Chem Eng*, 260 (2015) 291.
3 Diepgen L, Naldi L, Bruze M, Cazzaniga S, Schuttelaar L & Elsner P, *Invest Dermat*, 136 (2016) 409.
4 Jahn S, Faber H, Zazzeroni R & Karst U, *Rapid Commun Mass Spectr*, 26 (2012) 1453.
5 Breitwieser M, Viricel A, Churlaud C, Guillot B, Martin E & Stenger P L, *Comp Biochem Physiol Part C: Toxicol Pharmacol*, 199 (2017) 28 .
6 Ikarashi Y & Kaniwa A, *Health Sci*, 46 (2000) 467.
7 Meyer A, Blömeke B & Fischer K, *Chromatogr B*, 877 (2009) 1627.
8 Tokuda H, Kimura Y & Takano S, *Chromatogr*, 361 (1986) 345.
9 Stambouli A, Bellimam M, El Karni N, Bouayoun T & El Bouri A, *Forensic Sci Int*, 146 (2004) S87.
10 Stambouli A, Bellimam M A, El Karni N, Bouayoun T & El Bouri A, *Forensic Sci Int (Suppl)*, 146 (2004) S87.
11 Wang L H & Tsai S J, *Anal Biochem*, 312 (2003) 201.
12 Ngamdee K, Martwiset S, Tuntulani T & Ngeontae W, *Sensors Actuators B: Chem*, 173 (2012) 682.
13 Sasikumar R, Ranganathan P, Chen S M, Rwei S-P & Muthukrishnan, *J Colloid Interface Sci*, 504 (2017) 149.
14 Guo H L, Peng S, Xu J H, Zhao Y Q & Kang X, *Sensors Actuators B: Chem*, 193 (2014) 623.
15 Esfandiari Baghbamidi S, Beitollahi H & Tajik S, *Ionics*, 21 (2015) 2363.
16 Lu Y, Dong L, Jianshe H & Tianyan Y, *Sensors Actuators B: Chem*, 193 (2014) 166.
17 Hudari F F, de Almeida L C, Silva B F & Zanoni M B, *Microchem J*, 116 (2014) 261.
18 Thomas T, Mascarenhas R J, Martis P, Mekhalif Z & Swamy B K, *Mater Sci Engg: C*, 33 (2013) 3294.
19 Barsan M M, Ghica M E & Brett C A, *Anal Chim Acta*, 2670 (2015) 238.
20 Kim M S, Hsia B, Carraro C & Maboudian R, *Carbon*, 74 (2014) 163.
21 Suhas, Gupta V K, Carrott P M, Singh R, Chaudhary M & Kushwaha S, *Biores Technol*, 216 (2016)1066.
22 Valiūnienė A, Rekertaitė A I, Ramanavičienė A, Mikoliūnaitė L & Ramanavičius A, *Colloids Surfaces A: Physicochem Eng Aspects*, 7757 (2017) 30495.
23 Lee S H, Chung J H, Park H K & Lee G J, *J Sensors*, 2016 (2016) 1.
24 Zheng C, Zhou X F, Cao H L, Wang G H & Liu Z P, *J Power Sources*, 258 (2014) 290.
25 Hameed B H, Din A M & Ahmad A L, *J Hazard Mater*, 141 (2007) 819.
26 Tan I A W, Ahmad A L & Hameed B H, *J Hazard Mater*, 154 (2008) 337.
27 Asadollahi-Baboli M & Mani-Varnosfaderani A, *Measurement*, 47 (2014) 145.
28 Mažeikienė R, Niaura G & Malinauskas A, *EBSCO Ind*, 28 (2017) 28.
29 Martins A C, Pezoti O, Cazetta A L, Bedin K C, Yamazaki S & Bandoch G, *Chem Eng J*, 260 (2015) 291.
30 El Nemr A, El-Sikaily A, Khaled A & Abdelwahab O, *Arabian J Chem*, 8 (2015) 105.
31 Yamaguchi A, Inuzuka R, Takashima T, Hayashi T, Hashimoto K & Nakamura R, *Nature Commun,* 5 (2014) 4256.
32 Ribeiro D V & Abrantes J C, *Constr Build Mater,* 111 (2016) 98.
33 Gencoglu A & Minerick A R, *Microfluidics Nanofluidics*, 17 (2014) 781.
34 Bai Y H, Li J Y, Zhu Y h & Xu J J & Chen H Y, *Electroanalysis,* 22 (2010) 1239.
35 Dai S, Xu Z, Zhu M, Qian Y & Wang C, *Int J Electrochem Sci*, 10 (2015) 7063.
36 Zhu Y, Yan K, Liu Y & Zhang J, *Anal Chim Acta*, 884 (2015) 29.